Acta Crystallographica Section D
Biological Crystallography
ISSN 0907-4449

Alteration of fluorescent protein spectroscopic properties upon cryoprotection

David von Stetten,[a]* Gaëlle O. Batot,[a] Marjolaine Noirclerc-Savoye[b,c,d] and Antoine Royant[a,b,c,d]*

[a]Structural Biology Group, European Synchrotron Radiation Facility, Grenoble, France, [b]CNRS, Institut de Biologie Structurale, Grenoble, France, [c]CEA, Institut de Biologie Structurale, Grenoble, France, and [d]Université Joseph Fourier, Institut de Biologie Structurale, Grenoble, France

Correspondence e-mail: vonstett@esrf.fr, antoine.royant@ibs.fr

Received 15 May 2012
Accepted 4 September 2012

PDB Reference: Cerulean cryoprotected with EG, 4as8

Cryoprotection of a protein crystal by addition of small-molecule compounds may sometimes affect the structure of its active site. The spectroscopic and structural effects of the two cryoprotectants glycerol and ethylene glycol on the cyan fluorescent protein Cerulean were investigated. While glycerol had almost no noticeable effect, ethylene glycol was shown to induce a systematic red shift of the UV–vis absorption and fluorescence emission spectra. Additionally, ethylene glycol molecules were shown to enter the core of the protein, with one of them binding in close vicinity to the chromophore, which provides a sound explanation for the observed spectroscopic changes. These results highlight the need to systematically record spectroscopic data on crystals of light-absorbing proteins and reinforce the notion that fluorescent proteins must not been seen as rigid structures.

1. Introduction

The vast majority of protein X-ray structures are currently recorded at 100 K (as of April 2012, 89% of all X-ray entries in the PDB were recorded at temperatures below 130 K, as were 97% of structures deposited in 2011) in order to reduce radiation damage (Garman & Owen, 2006) and in some cases also to trap reaction intermediates (Bourgeois & Royant, 2005). However, the cryocooling process, which is usually performed in a nitrogen-gas stream or by plunging into liquid nitrogen, frequently disturbs the crystal lattice and thus degrades the diffracting power of the crystal. The main physical effect that damages the crystals during cryocooling is the volume contraction of the solvent during temperature changes, with or without the formation of ice crystals (Alcorn & Juers, 2010). Furthermore, different rates of contraction of the protein crystal and the surrounding solvent might cause additional strain on the crystal.

Therefore, it is recommended that the initial diffraction quality of a new protein crystal should be evaluated at room temperature (RT), even if collection of a complete data set may not be possible without severe radiation damage. This can be accomplished, for example, in capillaries or by using a humidifying device that prevents drying out of the crystal (Russi *et al.*, 2011; Wheeler *et al.*, 2012).

In order to record low-temperature diffraction data, a cryoprotecting agent can be added to the crystallization buffer to favour the formation of a vitreous or amorphous phase of the solvent instead of crystalline ice. Glycerol and ethylene glycol (EG or ethane-1,2-diol) are among the most commonly used cryoprotecting agents (Vera *et al.*, 2011). Other compounds used include low-molecular-weight PEGs, sucrose, salts and trimethylamine *N*-oxide (Mueller-Dieckmann *et al.*, 2011). Successful cryoprotection results in vitrification of the solvent, where the crystal order (and thus the diffracting power) is less disturbed, and the absence of crystalline ice avoids obscuring the protein diffraction pattern by ice rings. An efficient flash-cooling procedure usually yields transparent samples, thus allowing easier location of tiny crystals within a much larger drop of mother liquor. On the other hand, the addition of a cryoprotectant can in some cases lead to visible damage to the crystals (*e.g.* cracking or dissolving) even before flash-cooling, rendering them unsuitable

Table 1
Data-collection and refinement statistics for Cerulean cryoprotected with EG.

Values in parentheses are for the highest resolution shell.

Data collection	
Space group	$P2_12_12_1$
Unit-cell parameters (Å)	a = 51.3, b = 62.7, c = 70.2
X-ray source	ID29, ESRF
Wavelength (Å)	0.9793
Resolution (Å)	46.7–1.02 (1.08–1.02)
R_{merge} (%)	4.6 (35.7)
R_{meas} (%)	5.3 (45.6)
$\langle I/\sigma(I)\rangle$	14.3 (2.1)
Completeness (%)	96.9 (81.8)
Multiplicity	3.8 (2.0)
Refinement	
Resolution (Å)	46.8–1.02
R_{work}/R_{free} (%)	11.6/13.3
No. of atoms	
Total	2305
Protein	1962
Chromophore	27
Water	260
Ethylene glycol	56
B factors (Å^2)	
Overall	13.2
Protein	11.5
Chromophore	7.3
Water	25.1
Ethylene glycol	19.2
R.m.s. deviations	
Bond lengths (Å)	0.020
Bond angles (°)	2.2
PDB entry	4as8

for X-ray diffraction. Moreover, it has been reported that the presence of significant amounts of glycerol or EG corresponds to a considerable dehydration of the protein crystal (Wheeler *et al.*, 2012).

Unfortunately, in the typical setups used for flash-cooling in liquid nitrogen most of the cooling occurs in the gas layer above the liquid and blowing off this gas layer therefore increases the cooling rate by at least one order of magnitude (Warkentin *et al.*, 2006). The cooling rate is critical, as the sample has to be cooled to below the glass-transition temperature (130–160 K depending on the buffer composition) before nucleation of crystalline ice can occur (Kriminski *et al.*, 2002, 2003). The faster the cooling rate, the lower the concentration of cryoprotectant necessary to obtain a vitreous phase. As a further complication, all of these effects may be different inside and outside the protein crystal, which suggests the consideration of mixtures of a large-molecule cryoprotectant for the exterior solvent and a small-molecule cryoprotectant for the solvent channels for difficult cases (Alcorn & Juers, 2010).

Alternatively, the nylon loop or micromesh with the crystal can be swept through oil (*e.g.* paraffin, Paratone or perfluoroether; Garman & Owen, 2006). This effectively replaces the solvent around the crystal by oil, which unlike water does not crystallize at low temperatures. However, the oil does not penetrate the solvent channels and therefore only provides protection from harmful effects caused by volume changes of the surrounding liquid.

Last, but not least, it has recently been shown that flash-cooling without the use of additional compounds can also yield satisfactory results (especially when care is taken to minimize the amount of mother liquor surrounding the crystal) while avoiding most of the complications mentioned above and therefore this option should also be tried (Pellegrini *et al.*, 2011).

Owing to their small size and hydrophilic character, molecules of cryoprotecting agents are frequently found in X-ray structures of proteins. For instance, at the time of writing (April 2012), 9% of all protein X-ray structures in the PDB contain at least one glycerol molecule (three-letter code GOL) and 4% contain at least one EG molecule (three-letter code EDO). For example, glycerol or EG molecules have been identified in the active sites of various proteins (Sauvé *et al.*, 2009; Lehwess-Litzmann *et al.*, 2011; Yun *et al.*, 2009). In several cases, it has been shown that such embedded cryoprotectant molecules significantly affect the structure of active sites (Santos-Silva *et al.*, 2009; Brown *et al.*, 2009). Specifically, since glycerol resembles larger carbohydrates, it can be found in sugar-binding sites (Johal *et al.*, 2012; Wittmann *et al.*, 2008). Eventually, binding of cryoprotectant molecules can be turned into an ally for drug development or for enzymatic mechanism studies (Hung *et al.*, 2009; Lyubimov *et al.*, 2007).

As a consequence, ascertaining whether a cryoprotectant molecule might affect the structural analysis of a given mechanism is of prime importance. Unfortunately, only in rare cases are structures obtained with a different cryoprotectant or with no cryoprotectant agent available for comparison. Measuring the activity of a protein in solution in the absence or presence of cryoprotectant molecules is one possibile way of detecting severely detrimental effects, for example by studying the reaction kinetics of the protein. Successful avoidance of glycerol or EG molecules has been reported by using other cryoprotecting agents of greatly increased size (*e.g.* PEG 400; Scheuermann *et al.*, 2009) or of a different nature (*e.g.* magnesium sulfate; Transue *et al.*, 2004).

In this work, we report structural and spectroscopic changes induced by the common cryoprotectant EG in a cyan fluorescent protein (CFP). CFPs are derived from the green fluorescent protein (GFP) of the jellyfish *Aequorea victoria* and exhibit the same overall structure: an 11-strand β-barrel surrounding the chromophore, which is formed by the autocatalytic cyclization of three consecutive amino-acid residues. Their distinct blue-light absorption and cyan fluorescence emission properties are provided by a critical tyrosine-to-tryptophan mutation of the central residue of the chromophore (Heim & Tsien, 1996). Cerulean is a CFP with a fluorescence quantum yield of 49% (Rizzo *et al.*, 2004); its structure determination showed structural heterogeneity of the β-barrel next to the chromophore (Lelimousin *et al.*, 2009). Similar to other CFPs, Cerulean is mostly used in cell imaging as a donor to a yellow fluorescent protein in FRET-based cell-imaging experiments (Vogel *et al.*, 2006).

2. Experimental procedures

2.1. Protein expression, purification and crystallization

The protein was expressed, purified and crystallized as described previously (Lelimousin *et al.*, 2009). Cerulean crystals were obtained using the hanging-drop method at 293 K at a protein concentration of 13–16 mg ml^{-1} in 10–16%(v/v) PEG 8000, 100 mM $MgCl_2$, 100 mM HEPES pH 6.75–7.50.

2.2. Spectroscopy

UV–Vis absorption and fluorescence emission spectra were recorded in the Cryobench laboratory at the European Synchrotron Radiation Facility (ESRF), Grenoble, France (Royant *et al.*, 2007). To record crystal spectra at 100 K, crystals of 10–20 µm thickness were mounted in the nylon loops (Hampton Research) typically used for X-ray crystallography after washing them for a few seconds in mother liquor supplemented with either 30%(v/v) glycerol or EG. Solution spectra at 100 K were obtained using the same loops, which were filled with protein solution (optical path length ∼50 µm) after mixing with an equal amount of 30%(v/v) glycerol or EG. RT spectra were recorded from a sample sandwiched between two glass cover slips as

described previously (Royant *et al.*, 2007). For fluorescence excitation, a 440 nm laser (CrystaLaser) was used.

2.3. X-ray diffraction data collection and structure determination

Rather large single crystals of typically 200 µm in size were obtained. To cryoprotect crystals, they were washed for a few seconds in mother liquor mixed with 20%(*v*/*v*) glycerol or EG before flash-cooling in liquid nitrogen.

Diffraction data sets were obtained on beamline ID29 at the ESRF (de Sanctis *et al.*, 2012) using the helical data-collection mode to minimize radiation damage (Flot *et al.*, 2010). The data were integrated with *XDS* (Kabsch, 2010) and scaled and merged with *SCALA* (Collaborative Computational Project, Number 4, 1994; Evans, 2006; Winn *et al.*, 2011). The 1.15 Å resolution structure of Cerulean (PDB entry 2wso; Lelimousin *et al.*, 2009) was used as starting model for refinement with *REFMAC* (Collaborative Computational Project, Number 4, 1994; Murshudov *et al.*, 2011; Winn *et al.*, 2011). Initially, all anisotropic *B* factors were reset to isotropic *B* factors and calculated again after the first round of refinement. *Coot* (Emsley *et al.*, 2010) was used for inspection and modification of the calculated models. Data-reduction and structure-refinement statistics are shown in Table 1. The structure and structure-factor amplitudes of Cerulean cryoprotected with EG have been deposited in the PDB (http://www.pdb.org/) as entry 4as8. Structure figures were prepared with *PyMOL* (http://www.pymol.org/).

3. Results and discussion

Initial structure determination of CFP mutants was performed using glycerol as a cryoprotectant (Lelimousin *et al.*, 2009). The observation that the crystals were cracking at some point during equilibration with mother liquor supplemented with glycerol prompted us to try a new cryoprotectant. EG was suggested since we were using PEG as a precipitant. Crystals seemed to survive better in the crystallization drop with EG and the diffraction limits were of the same order of magnitude. However, it occurred to us that EG-cryoprotected crystals seemed to be more radiation-sensitive than glycerol-cryoprotected crystals, as indicated by a systematic negative peak located on residue Glu222 in $F_o - F_c$ difference maps. This feature was the first

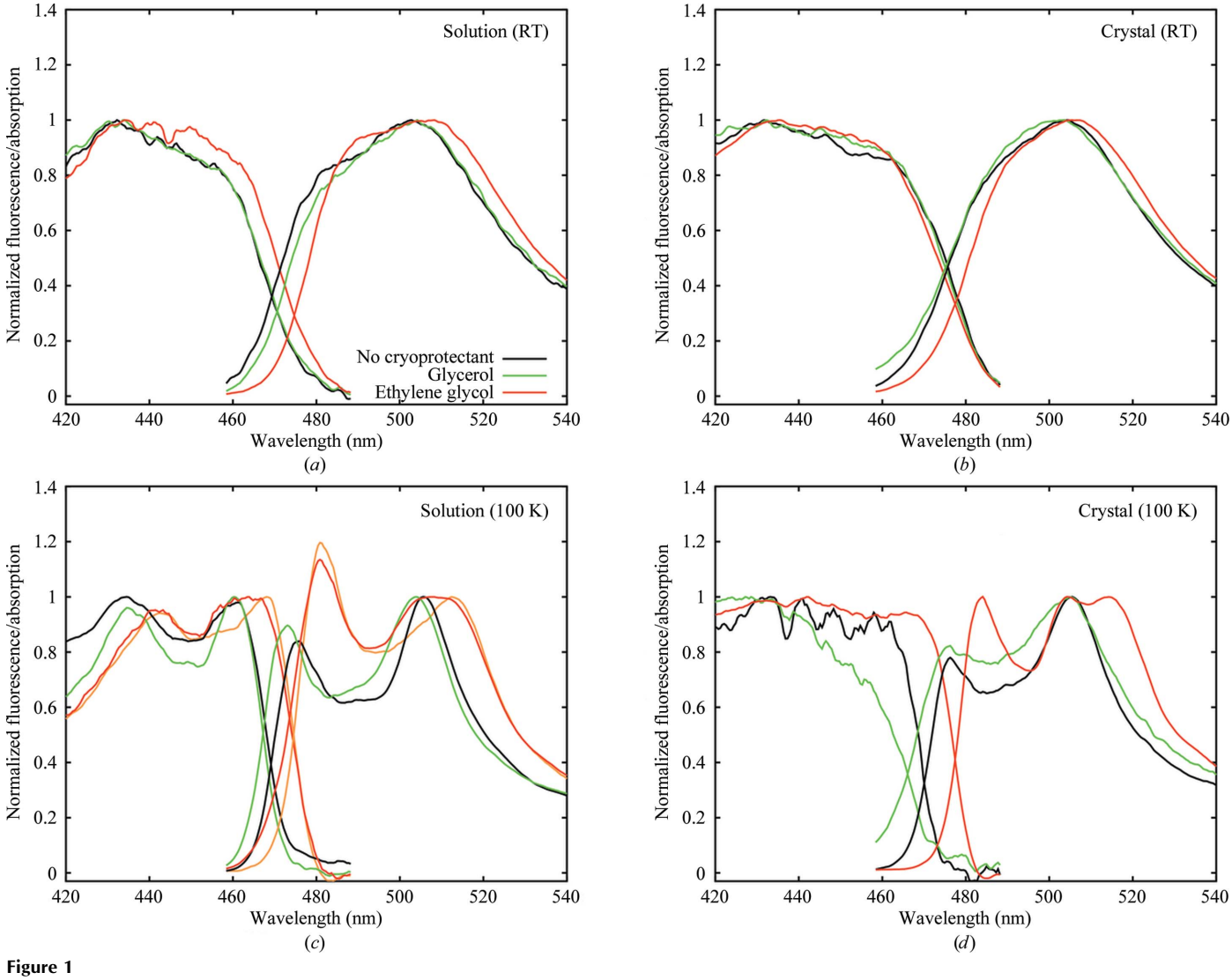

Figure 1
UV–Vis absorption and fluorescence spectra of Cerulean solution and crystals recorded after addition of EG (red) or glycerol (green) or in in regular buffer (black). In (*c*), spectra recorded at a higher EG concentration [80%(*v*/*v*)] are addditionally shown (orange). Spectra were recorded at RT or 100 K and are normalized. Note: several crystal absorption spectra are rather noisy near 420–460 nm owing to saturation effects caused by the high optical density of the crystals.

feature to be observed during radiation-damage studies of enhanced green fluorescent protein (Royant & Noirclerc-Savoye, 2011) and various CFPs (unpublished data). These systematic differences prompted us to measure the absorption and fluorescence emission spectra of variously cryoprotected crystals, which made us immediately aware of the effect of EG and drove our reinterpretation of the structural data. The spectroscopic and structural effects of cryoprotectants will be detailed in the next two sections.

3.1. Spectroscopic effects of cryoprotectants

The CFP Cerulean exhibits double-peaked absorption and fluorescence emission spectra, which are characteristic of fluorescent proteins with a tryptophan as the central residue of the chromophore (Shaner *et al.*, 2004). We systematically recorded spectra of Cerulean samples under various temperature, phase and cryoprotection conditions: at 100 K or RT, from purified protein solutions or crystals and with or without the addition of glycerol or EG (Fig. 1).

The most striking observation is the fact that the presence of EG leads to a significant red shift of absorption and fluorescence peaks under all conditions when compared with the noncryoprotected case. Because the width of the spectroscopic peaks decreases with temperature, the EG-induced red shift can be better seen in spectra recorded at 100 K (Figs. 1*c* and 1*d*). Specifically, solution samples that were flash-cooled at 100 K without cryoprotectant exhibited fluorescence emission peaks at 475 and 505 nm. When EG was added, the shorter wavelength emission peak shifted by 5 nm to 480 nm, while the longer wavelength peak was also red-shifted and was roughly twice as broad. The two absorption bands were similarly red-shifted in the presence of EG. The situation was identical in the crystalline state (Figs. 1*b* and 1*d*) but, presumably because of the reduced conformational freedom in the crystalline state, the broadened emission peak in the crystal EG spectra was resolved as a double peak at 504 and 514 nm at 100 K in addition to the peak at 484 nm. Similar results were obtained at RT. Interestingly, spectra of Cerulean recorded in a buffer with 80%(*v*/*v*) EG showed a more extreme case in which the peak at 504 nm disappeared and only the shifted peak at 514 nm remained (orange spectrum in Fig. 1*c*). It should be noted that the shorter wavelength part of the emission spectra could be reabsorbed by the surrounding molecules (Figs. 1*c* and 1*d*), especially in the highly concentrated crystalline state (Barros *et al.*, 2009). Therefore, the precise position of the shorter wavelength emission peak cannot be determined reliably.

Conversely, the presence of glycerol had no detectable spectroscopic effect when compared with the noncryoprotected case in all but one of four conditions (*i.e.* solutions at 100 K), in which the peaks in the presence of glycerol were slightly blue shifted by 2 nm to 473 and 503 nm (Fig. 1*c*).

3.2. Structural effects of cryoprotectants

In light of the observed spectroscopic differences, we carefully investigated the changes observed in crystals that were either flash-cooled without cryoprotectant following the method described by Pellegrini *et al.* (2011) or after the addition of 20%(*v*/*v*) EG to the mother liquor compared with the previously published Cerulean structure obtained from glycerol-cryoprotected crystals (Lelimousin *et al.*, 2009). No structural change could be identified in the noncryoprotected structure (data not shown), suggesting that glycerol-cryoprotected structures show the physiological state of the protein.

In contrast, several changes were identified in the EG-cryoprotected structure. Foremost, nine well ordered EG molecules were found at the surface of the protein (Fig. 2*c*), generally replacing two neighbouring water molecules observed in the glycerol-cryoprotected and noncryoprotected Cerulean structures. The key feature to identify EG molecules is their characteristic asymmetric residual density when modelled as two water molecules (Figs. 2*a*, 2*b*, 2*d* and 2*f*).

In particular, one of these EG molecules induced a reorientation of the side chains of Tyr39 and Arg122. More interestingly, two EG molecules were found within the seemingly rigid β-barrel (Fig. 2*c*). The first one replaces two water molecules at a distance of about 7 Å from the chromophore. The second one is located very close (3 Å) to the chromophore, as indicated by the residual $F_o - F_c$ electron density after initial refinement cycles of the structure (Fig. 2*d*). It only partially replaces two of the water molecules; as a consequence, it partially displaces the side chains of residues Thr65 and Glu222 by its larger bulk, because the C atoms of the EG molecule obviously prevent the hydrogen bond between Glu222 and one hydroxyl group of the EG molecule (Figs. 2*e* and 2*f*). Therefore, the negative electron density observed on the side chain of Glu222, which had originally been misinterpreted as radiation damage, in fact arises from EG-induced conformational changes of this residue. The occupancies of the EG molecule and of the alternate conformation of Glu222 were estimated to be 50 ± 5%, while that of the alternate conformation of Thr65 was estimated to be 25 ± 5%.

3.3. Discussion

Distinct spectroscopic effects were observed in samples of the fluorescent protein Cerulean upon the addition of glycerol or EG. Even rather small peak shifts, such as those described above, could degrade the data quality of experiments that rely on the evaluation of the fluorescence emission intensity at a given wavelength. Therefore, it is of great interest to understand the underlying mechanisms that lead to such effects, as in principle other molecules that occur in cells could have similar consequences.

In protein crystals and RT solutions glycerol does not affect the absorption and emission spectra of Cerulean, but in solutions at 100 K a small but reproducible blue shift is observed. This phenomenon is reminiscent of the observation that glycerol affects the fluorescence lifetime of fluorescent proteins *via* a change in the refractive index of the surrounding medium (Borst *et al.*, 2005; Suhling *et al.*, 2002), which is different for glycerol (n = 1.47 at RT), EG (n = 1.43 at RT) and water (n = 1.33 at RT) (Spangler & Davies, 1943; Refractive Index Database, http://refractiveindex.info/). Therefore, we can only speculate that the small blue shift of both emission peaks under this specific condition might be related to the differing refractive index of the medium. It is unclear to us why this does not play a role under other conditions.

In contrast, addition of EG results in a systematic and significant red shift under all experimental conditions. EG molecules were found within the core of the protein at a relatively close distance to the chromophore. In particular, one binding site right next to the chromophore induces significant structural changes in a few nearby residues, which are likely to account for the observed spectroscopic red shift. Specifically, the negatively charged residue Glu222 moves away from the chromophore. Alternatively or additionally, the EG molecule could directly affect the energy levels of the chromophore; this would have to be tested using quantum-mechanical calculations.

The occupancy of the EG molecule next to the chromophore is only 50%, which offers a fitting explanation for the broadening or the doubling of the fluorescence emission peak (Figs. 1*c* and 1*d*). In addition to an unchanged spectral species (emission peak at 504 nm), an equally strong contribution with a shifted emission peak appears, resulting in a broadened peak (solutions at 100 K) or a double peak

at 504/514 nm (crystals at 100 K). The further increased intensity of the red-shifted part of the fluorescence spectrum upon the addition of 80%(*v*/*v*) glycerol confirms this mechanism.

Part of the Cerulean structure between the chromophore and the bulk solvent has previously been observed in alternate conformations, which were interpreted as medium-scale movements of a single β-strand (Lelimousin *et al.*, 2009). Although it would have been tempting to relate this dynamic disorder to the entry of EG molecules inside the protein, the fact that all of the results reported here were reproduced on solutions and crystals of mTurquoise, for which the dynamics of the strand have mostly been eliminated (Goedhart *et al.*, 2010, 2012), shows that the apparently rigid structure of fluorescent proteins naturally exhibits breathing modes which allow molecules significantly larger than water molecules to approach the chromophore. In particular, this can explain why fluorescent proteins, which were thought to protect their chromophore from interactions with the solvent, have been shown to act as type I or type II photosensitizers (Bulina *et al.*, 2006; Jiménez-Banzo *et al.*, 2008; Serebrovskaya *et al.*, 2009), *i.e.* molecular oxygen can diffuse to the chromophore.

We have shown that the cryoprotectant EG binds within the protein and interacts with the chromophore, thus affecting its spectroscopic properties. Because both the structural and the spectroscopic changes are moderate, they could easily go unnoticed but nevertheless lead to misinterpretation of the data. An obvious result is the suggestion that glycerol rather than EG should preferentially be used as a cryoprotectant in work with fluorescent proteins at low temperatures. Furthermore, this example reinforces the notion that any crystalline protein with a spectroscopic signature in the visible-light range needs to be systematically investigated by UV–visible absorption (or fluorescence or Raman) spectroscopy in order to ensure that the state of the protein as observed in the crystal structure relates as closely as possible to that in solution.

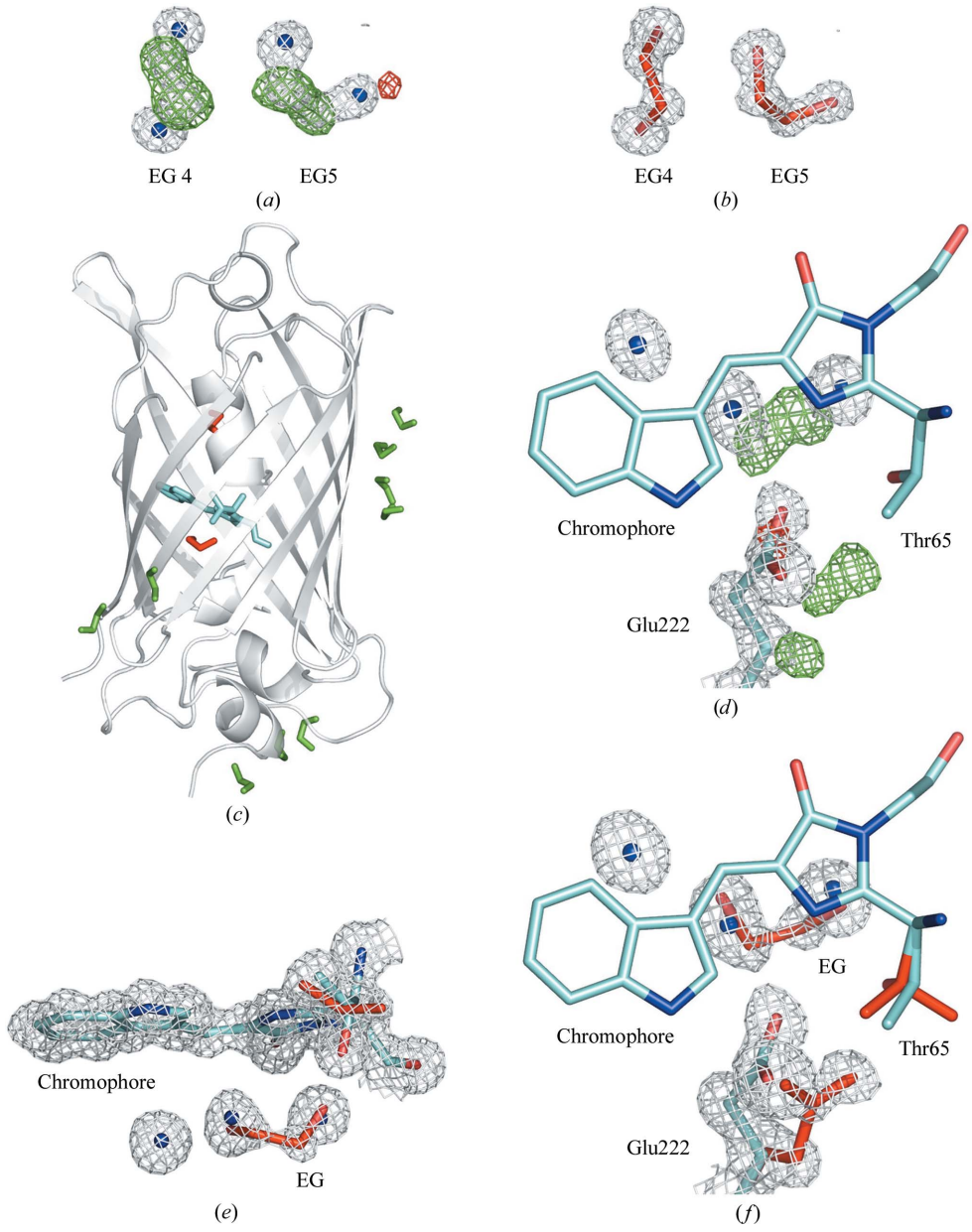

Figure 2
Structure of EG-cryoprotected Cerulean. (*a*) Two EG-binding sites near Pro192 after refinement with the glycerol-cryoprotected structure of Cerulean (PDB entry 2wso); $F_o - F_c$ (green and red) and $2F_o - F_c$ (grey) electron densities are contoured at $\pm 3.5\sigma$ and 1.6σ, respectively. (*b*) The same electron density as in (*a*) but modelled as two EG molecules (contoured at 1.6σ). (*c*) Nine EG molecules were found at the surface of the protein (green) and two were found inside the β-barrel (red). (*d*) $F_o - F_c$ (green and red) and $2F_o - F_c$ (grey) electron densities contoured at $\pm 3.5\sigma$ and 1.5σ, respectively, near the chromophore (light blue) after refinement with the glycerol-cryoprotected structure of Cerulean (PDB entry 2wso), *i.e.* with three water molecules (dark blue) nearby. (*e*, *f*) The residual electron density could be successfully modelled by alternate conformations (red) of Thr65 and Glu222 as well as a partially occupied EG molecule, as shown by the $2F_o - F_c$ electron density contoured at a $\pm 0.7\sigma$ level. (*f*) 90° rotated view of (*e*) with Glu222 and without $2F_o - F_c$ electron density of the chromophore.

The Structural Biology group of the ESRF is gratefully acknowledged for their help. We are grateful to D. de Sanctis, J. Goedhart and T. W. Gadella Jr for helpful discussions. The Partnership for Structural Biology is acknowledged for access to the RoBioMol and Cryobench platforms. AR acknowledges financial support from the ANR (ANR-11-JSV5-0009-01).

References

Alcorn, T. & Juers, D. H. (2010). *Acta Cryst.* D**66**, 366–373.
Barros, T., Royant, A., Standfuss, J., Dreuw, A. & Kühlbrandt, W. (2009). *EMBO J.* **28**, 298–306.

Borst, J. W., Hink, M. A., van Hoek, A. & Visser, A. J. (2005). *J. Fluoresc.* **15**, 153–160.
Bourgeois, D. & Royant, A. (2005). *Curr. Opin. Struct. Biol.* **15**, 538–547.
Brown, C. J., Verma, C. S., Walkinshaw, M. D. & Lane, D. P. (2009). *Cell Cycle*, **8**, 1905–1911.
Bulina, M. E., Chudakov, D. M., Britanova, O. V., Yanushevich, Y. G., Staroverov, D. B., Chepurnykh, T. V., Merzlyak, E. M., Shkrob, M. A., Lukyanov, S. & Lukyanov, K. A. (2006). *Nature Biotechnol.* **24**, 95–99.
Collaborative Computational Project, Number 4 (1994). *Acta Cryst.* D**50**, 760–763.
Emsley, P., Lohkamp, B., Scott, W. G. & Cowtan, K. (2010). *Acta Cryst.* D**66**, 486–501.
Evans, P. (2006). *Acta Cryst.* D**62**, 72–82.
Flot, D., Mairs, T., Giraud, T., Guijarro, M., Lesourd, M., Rey, V., van Brussel, D., Morawe, C., Borel, C., Hignette, O., Chavanne, J., Nurizzo, D., McSweeney, S. & Mitchell, E. (2010). *J. Synchrotron Rad.* **17**, 107–118.
Garman, E. F. & Owen, R. L. (2006). *Acta Cryst.* D**62**, 32–47.
Goedhart, J., van Weeren, L., Hink, M. A., Vischer, N. O., Jalink, K. & Gadella, T. W. Jr (2010). *Nature Methods*, **7**, 137–139.
Goedhart, J., von Stetten, D., Noirclerc-Savoye, M., Lelimousin, M., Joosen, L., Hink, M. A., van Weeren, L., Gadella, T. W. Jr & Royant, A. (2012). *Nature Commun.* **3**, 751.
Heim, R. & Tsien, R. Y. (1996). *Curr. Biol.* **6**, 178–182.
Hung, A. W., Silvestre, H. L., Wen, S., Ciulli, A., Blundell, T. L. & Abell, C. (2009). *Angew. Chem. Int. Ed. Engl.* **48**, 8452–8456.
Jiménez-Banzo, A., Nonell, S., Hofkens, J. & Flors, C. (2008). *Biophys. J.* **94**, 168–172.
Johal, A. R., Schuman, B., Alfaro, J. A., Borisova, S., Seto, N. O. L. & Evans, S. V. (2012). *Acta Cryst.* D**68**, 268–276.
Kabsch, W. (2010). *Acta Cryst.* D**66**, 125–132.
Kriminski, S., Caylor, C. L., Nonato, M. C., Finkelstein, K. D. & Thorne, R. E. (2002). *Acta Cryst.* D**58**, 459–471.
Kriminski, S., Kazmierczak, M. & Thorne, R. E. (2003). *Acta Cryst.* D**59**, 697–708.
Lehwess-Litzmann, A., Neumann, P., Parthier, C., Lüdtke, S., Golbik, R., Ficner, R. & Tittmann, K. (2011). *Nature Chem. Biol.* **7**, 678–684.
Lelimousin, M., Noirclerc-Savoye, M., Lazareno-Saez, C., Paetzold, B., Le Vot, S., Chazal, R., Macheboeuf, P., Field, M. J., Bourgeois, D. & Royant, A. (2009). *Biochemistry*, **48**, 10038–10046.
Lyubimov, A. Y., Heard, K., Tang, H., Sampson, N. S. & Vrielink, A. (2007). *Protein Sci.* **16**, 2647–2656.
Mueller-Dieckmann, C., Kauffmann, B. & Weiss, M. S. (2011). *J. Appl. Cryst.* **44**, 433–436.
Murshudov, G. N., Skubák, P., Lebedev, A. A., Pannu, N. S., Steiner, R. A., Nicholls, R. A., Winn, M. D., Long, F. & Vagin, A. A. (2011). *Acta Cryst.* D**67**, 355–367.
Pellegrini, E., Piano, D. & Bowler, M. W. (2011). *Acta Cryst.* D**67**, 902–906.
Rizzo, M. A., Springer, G. H., Granada, B. & Piston, D. W. (2004). *Nature Biotechnol.* **22**, 445–449.
Royant, A., Carpentier, P., Ohana, J., McGeehan, J., Paetzold, B., Noirclerc-Savoye, M., Vernède, X., Adam, V. & Bourgeois, D. (2007). *J. Appl. Cryst.* **40**, 1105–1112.
Royant, A. & Noirclerc-Savoye, M. (2011). *J. Struct. Biol.* **174**, 385–390.
Russi, S., Juers, D. H., Sanchez-Weatherby, J., Pellegrini, E., Mossou, E., Forsyth, V. T., Huet, J., Gobbo, A., Felisaz, F., Moya, R., McSweeney, S. M., Cusack, S., Cipriani, F. & Bowler, M. W. (2011). *J. Struct. Biol.* **175**, 236–243.
Sanctis, D. de *et al.* (2012). *J. Synchrotron Rad.* **19**, 455–461.
Santos-Silva, T., Ferroni, F., Thapper, A., Marangon, J., González, P. J., Rizzi, A. C., Moura, I., Moura, J. J. G., Romão, M. J. & Brondino, C. D. (2009). *J. Am. Chem. Soc.* **131**, 7990–7998.
Sauvé, V., Roversi, P., Leath, K. J., Garman, E. F., Antrobus, R., Lea, S. M. & Berks, B. C. (2009). *J. Biol. Chem.* **284**, 21707–21718.
Scheuermann, T. H., Tomchick, D. R., Machius, M., Guo, Y., Bruick, R. K. & Gardner, K. H. (2009). *Proc. Natl Acad. Sci. USA*, **106**, 450–455.
Serebrovskaya, E. O., Edelweiss, E. F., Stremovskiy, O. A., Lukyanov, K. A., Chudakov, D. M. & Deyev, S. M. (2009). *Proc. Natl Acad. Sci. USA*, **106**, 9221–9225.
Shaner, N. C., Campbell, R. E., Steinbach, P. A., Giepmans, B. N., Palmer, A. E. & Tsien, R. Y. (2004). *Nature Biotechnol.* **22**, 1567–1572.
Spangler, J. & Davies, E. (1943). *Ind. Eng. Chem. Anal. Ed.* **15**, 96–99.
Suhling, K., Siegel, J., Phillips, D., French, P. M., Lévêque-Fort, S., Webb, S. E. & Davis, D. M. (2002). *Biophys. J.* **83**, 3589–3595.
Transue, T. R., Krahn, J. M., Gabel, S. A., DeRose, E. F. & London, R. E. (2004). *Biochemistry*, **43**, 2829–2839.
Vera, L., Czarny, B., Georgiadis, D., Dive, V. & Stura, E. A. (2011). *Cryst. Growth Des.* **11**, 2755–2762.
Vogel, S. S., Thaler, C. & Koushik, S. V. (2006). *Sci. STKE*, **2006**, re2.
Warkentin, M., Berejnov, V., Husseini, N. S. & Thorne, R. E. (2006). *J. Appl. Cryst.* **39**, 805–811.
Wheeler, M. J., Russi, S., Bowler, M. G. & Bowler, M. W. (2012). *Acta Cryst.* F**68**, 111–114.
Winn, M. D. *et al.* (2011). *Acta Cryst.* D**67**, 235–242.
Wittmann, J. G., Heinrich, D., Gasow, K., Frey, A., Diederichsen, U. & Rudolph, M. G. (2008). *Structure*, **16**, 82–92.
Yun, S.-M. *et al.* (2009). *Nature Struct. Mol. Biol.* **16**, 876–882.